Dynamical quantum filtering in the scattering dynamics of H_2 on Cu(001)

2002 J. Phys.: Condens. Matter 14 L479

(http://iopscience.iop.org/0953-8984/14/25/107)

INSTITUTE OF PHYSICS PUBLISHING JOURNAL OF PHYSICS: CONDENSED MATTER

J. Phys.: Condens. Matter **14** (2002) L479–L486 PII: S0953-8984(02)37050-4

LETTER TO THE EDITOR

Dynamical quantum filtering in the scattering dynamics of H_2 on Cu(001)

Yoshio Miura[1,2], **Hideaki Kasai**[2] **and Wilson Agerico Diño**[2,3]

[1] Japan Science and Technology, Kawaguchi, Saitama, 332-0012, Japan
[2] Department of Applied Physics, Osaka University, Suita, Osaka, 565-0871, Japan
[3] Institute of Industrial Science, The University of Tokyo, Komaba, Meguro-ku, Tokyo, 153-8505, Japan

E-mail: miura@dyn.ap.eng.osaka-u.ac.jp

Received 15 May 2002
Published 14 June 2002
Online at stacks.iop.org/JPhysCM/14/L479

Abstract

We investigate and discuss the effects of dynamical quantum filtering on the scattering dynamics of H_2 on Cu(001); we perform coupled-channel calculations, including all six degrees of freedom of H_2, on an *ab initio* potential energy surface. Our results show that cartwheel-like rotating H_2 molecules (with their angular momentum vectors $\boldsymbol{j}$ predominantly oriented parallel to the surface) exhibit strong specular scattering on Cu(001), while helicopter-like rotating H_2 molecules (with their angular momentum vectors $\boldsymbol{j}$ predominantly oriented perpendicular to the surface) exhibit off-specular scattering on Cu(001). These results indicate that we can obtain H_2 molecules with aligned angular momentum vectors $\boldsymbol{j}$, by scattering them from solid surfaces.

Investigations of hydrogen–surface reactions are essential for obtaining a fundamental understanding of dynamical processes occurring on solid surfaces, and achieving efficient control of industrially important gas–surface reactions. One of the experimental approaches which has been developed to investigate hydrogen–surface reactions over recent years is that of measuring the energy distributions of hydrogen molecules desorbing/scattering from the surface, because the desorbing and scattering molecules carry a lot of information concerning the hydrogen–surface interactions. By detecting the molecules using state-specific probes, such as the *time-of-flight* (TOF) mass spectrometer [1–9], *resonance-enhanced multiphoton ionization* (REMPI) [2, 4–11], and *laser-induced fluorescence* (LIF) detection techniques [12, 13], it is possible to determine the angle-resolved translational distributions, internal (rotational and vibrational) state distributions, and orientational preferences of hydrogen molecules. Experimental studies, as well as quantum dynamics calculations on *ab initio* potential energy surfaces (PES) [14–23], have greatly contributed to our understanding of the mechanisms of energy flow and energy disposal in hydrogen–surface reactions from a

microscopic point of view. (Interested readers are referred to recent reviews of experimental and theoretical works on hydrogen–surface reactions [24–29].)

Recently, we reported on the dynamical quantum filtering (DQF) effects on the associative desorption dynamics of H_2 from metal surfaces [30–32]. For low final translational energies, desorbing H_2 exhibit a preference for cartwheel-like rotation (angular momenta $\boldsymbol{j}$ predominantly oriented parallel to the surface). On the other hand, for high final translational energies, desorbing H_2 exhibit a preference for helicopter-like rotation (angular momenta $\boldsymbol{j}$ predominantly oriented perpendicular to the surface). These results indicate that we can obtain H_2 having aligned angular momentum vectors $\boldsymbol{j}$ through the associative desorption of H_2. Then, using DQF, we designed a reaction procedure that enhances/increases the *ortho*-H_2–*para*-H_2 (*o*–*p* H_2) conversion yield [33]. Recently, we also found that the *o*–*p* H_2 conversion probabilities for a cartwheel-like rotating H_2 are around one order of magnitude higher than those for a helicopter-like rotating H_2 [34–36]. This strong steric effect, when combined with DQF, enables us to increase the *o*–*p* H_2 conversion yield. We first obtain H_2 having aligned angular momentum vectors $\boldsymbol{j}$ by the use of DQF through the associative desorption of H_2 from surfaces. We then bring these aligned H_2 close to a catalyst surface (e.g., a metal oxide surface) in such a way that H_2 interacting with the surface are always exhibiting cartwheel-like rotation. We can thus obtain a high *o*–*p* H_2 conversion rate, due to the steric effect.

In this letter, we focus on the DQF effect on the scattering dynamics of H_2 on Cu(001). We found that we can also align the angular momentum vectors $\boldsymbol{j}$ of H_2 through the process of scattering on the surface. To demonstrate and explain how the angular momentum vectors $\boldsymbol{j}$ of H_2 are aligned during the scattering on metal surfaces, we perform full quantum dynamics calculations for H_2 on Cu(001), taking into account all six degrees of freedom of H_2 as dynamical variables, and using the time-independent coupled-channel method.

The dynamical variables that we have considered are the perpendicular distance of the H_2 centre of mass from the surface Z, the H_2 centre-of-mass position parallel to the surface (X, Y), the H_2 bond length r, and the H_2 polar and azimuthal orientations with respect to the surface, θ and ϕ, respectively. We then make a transformation from the Cartesian coordinate system to the mass-weighted reaction path coordinate system [37]. Here, we leave the details of the derivation to [38], and show only the final form of the Hamiltonian, which is given by

$$H = -\frac{\hbar^2}{2M}\left[\frac{\partial^2}{\partial X^2} + \frac{\partial^2}{\partial Y^2}\right] - \frac{\hbar^2}{2\mu}\left[\eta^{-1}\frac{\partial}{\partial v}\eta\frac{\partial}{\partial v}\right] + \frac{\hbar^2}{2\mu}\frac{1}{r}L\frac{1}{r} + V(X, Y, s, \theta, \phi, v). \tag{1}$$

M and μ are the total and reduced masses of H_2. s corresponds to the reaction path coordinate along the potential minimum on a PES, and v corresponds to the vibrational coordinate perpendicular to the reaction path. L is the angular momentum operator. η is the Jacobian of the transformation $\eta(s, v, \theta) = 1 - vC(s, \theta)$, where $C(s, \theta)$ is the reaction path curvature. $V(X, Y, s, \theta, \phi, v)$ gives the six-dimensional (6D) PES along the reaction path for H_2/Cu(001). Since the hydrogen–copper system has been studied extensively, large amounts of information are now available on the PES of the hydrogen–copper system [39–42]. An analytical functional form of the 6D PES of H_2 on the $\{100\}$ face of copper fitted to the PES calculation results based on density functional theory (DFT) obtained for the highly symmetric sites was earlier given by Wiesenekker *et al* [39] in the Cartesian coordinate system. Here, we show the corresponding functional form in the mass-weighted reaction path coordinate system:

$$\begin{aligned} V(X, Y, s, \theta, \phi, v) = {} & V_{0000}(s) + V_{0010}(s)[\cos GX + \cos GY] + V_{0011}(s)[\cos GX \cos GY] \\ & + V_{2000}(s)\cos^2\theta + V_{2010}(s)\cos^2\theta[\cos GX + \cos GY] \\ & + V_{2011}(s)\cos^2\theta[\cos GX \cos GY] \\ & + V_{2210}(s)\sin^2\theta\cos 2\phi[\cos GX - \cos GY] + \tfrac{1}{2}\mu\omega^2(s)v^2. \end{aligned} \tag{2}$$

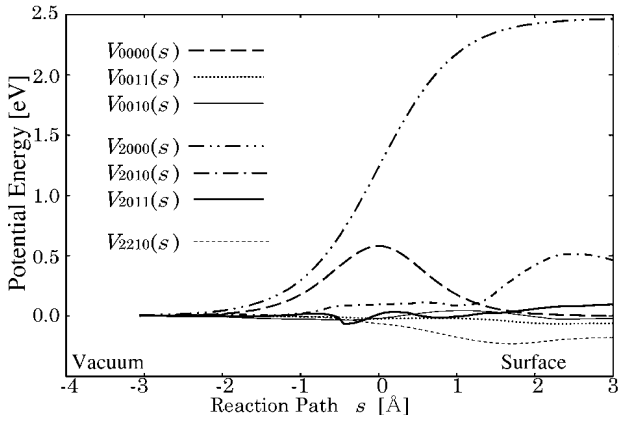

Figure 1. Coefficients V_{mnjm_j} of the expansion of the 6D PES, $V(X, Y, s, \theta, \phi, v)$, used in the present calculation along the reaction path s.

Each $V_{jm_jmn}(s)$ corresponds to the s-dependent coefficients of the expansion of the 6D PES (here, $V_{jm_jmn}(s) = V_{jm_jnm}(s)$). m and n are the quantum numbers for the surface-parallel translational motion of H_2, and correspond to the diffraction channels. j and m_j are quantum numbers for the rotational motion of H_2, and j corresponds to the absolute value of the angular momentum vector $\boldsymbol{j}$ while m_j corresponds to the surface-normal component of the angular momentum vector $\boldsymbol{j}$. $G = 2\pi/a$ is the reciprocal-lattice constant of the surface unit cell of Cu(001). $a = 2.55$ Å is the nearest-neighbour distance between Cu atoms on the surface. $\omega(s)$ corresponds to the vibrational frequency of the adsorbed H ($s = -\infty$) and the vibrational frequency of the desorbing H_2 ($s = \infty$). Equation (2) reproduces the same PES for H_2/Cu(001) as those of [39]. In figure 1, we show each $V_{jm_jmn}(s)$ in equation (2) as a function of the reaction path coordinate s. The wavefunction is expanded in terms of two-dimensional plane waves in X and Y, harmonic oscillator functions $\beta_v(s, v)$, and spherical harmonic functions $Y_j^{m_j}(\theta, \phi)$, i.e.,

$$\Psi(s, v, X, Y, \theta, \phi) = \sum_{mnvjm_j} \phi_{mnv}^{jm_j}(s) \exp[-\mathrm{i}G(mX + nY)]\beta_v(s, v)Y_j^{m_j}(\theta, \phi). \tag{3}$$

v is the quantum number for the vibrational motion of product H_2. The size of the basis set used in the coupled-channel calculations is determined by the total energy of the system E_{tot}, which is defined as the sum of the kinetic energy of the surface-normal translational motion, surface-parallel translational motion, rotational motion, and vibrational motion of H_2. When the maximum $E_{tot} = 0.4$ [eV], the calculation results converge with maximum quantum numbers $j_{max} = 5$, $v_{max} = 1$, and $G_{max} = 8$. We carefully checked the convergence for calculations with maximum quantum numbers $j_{max} = 7$, $v_{max} = 2$, and $G_{max} = 9$.

We calculate the scattering probabilities $R_{mnjm_j}^{m'n'}(E_{tot})$ as functions of final states of the rotational motion (j, m_j), and initial (m', n') and final (m, n) states of the surface-parallel translational motions of H_2 for the scattering dynamics on Cu(001). Note that in evaluating the $R_{mnjm_j}^{m'n'}(E_{tot})$, we summed the results over all possible initial rotational states of impinging H_2 (j', m'_j), and we fixed the initial and final vibrational states of H_2 at the ground state. In figure 2, we show the surface-parallel wavevector $(G(m, n))$ distributions for cartwheel-like rotating H_2 $(j = 1, m_j = 0)$ and helicopter-like rotating H_2 $(j = 1, |m_j| = 1)$ scattered from Cu(001), in the case of $E_{tot} = 0.2$ [eV]. In figures 2(a) and (b), the surface-parallel wavevector of the impinging H_2 is fixed at $\boldsymbol{K}_i = G(1, 0)$ along the [100] direction of Cu(001), which corresponds

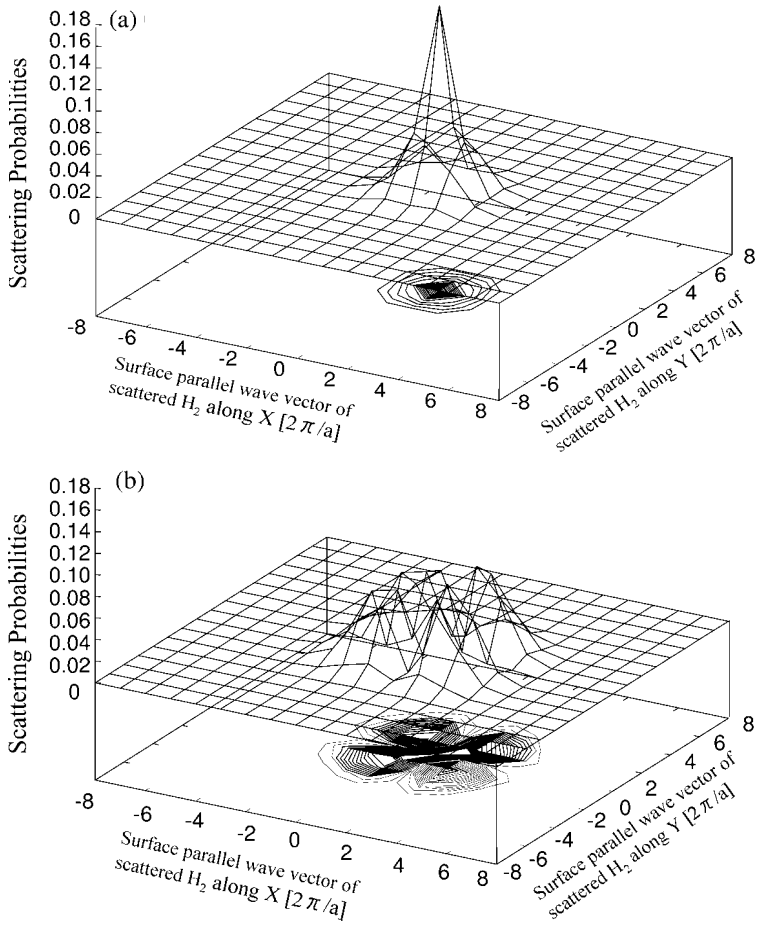

Figure 2. Distributions of the surface-parallel wavevector $G(m, n)$ ($G = 2\pi/a$, $a = 2.55$ (Å)) for (a) a cartwheel-like rotating H_2 ($j = 1, m_j = 0$) and (b) a helicopter-like rotating H_2 ($j = 1, |m_j| = 1$) scattered from Cu(001), in the vibrational ground state ($v = 0$) for the case when $E_{tot} = 0.2$ [eV].

to an incident angle $\Theta_i \approx 10°$ with respect to the surface normal for $E_{tot} = 0.2$ [eV]. As we can see in figure 2, the angular distributions of the cartwheel-like rotating H_2 (figure 2(a)) are quite different from those of the helicopter-like rotating H_2 (figure 2(b)). The cartwheel-like rotating H_2 exhibit strong specular scattering, i.e., there is a sharp peak at $\boldsymbol{K}_f = \boldsymbol{K}_i$, while the helicopter-like rotating H_2 exhibit off-specular scattering, i.e., there is no peak at $\boldsymbol{K}_f = \boldsymbol{K}_i$; instead, there are small peaks around $\boldsymbol{K}_f = \boldsymbol{K}_i$. $\boldsymbol{K}_f$ corresponds to the surface-parallel wavevector of scattered H_2.

These results can be understood in terms of the coupling between the surface-parallel translational motion and the rotational motion of H_2. When the H_2 impinges on the surface, the corrugation (dependence on X and Y) of the PES and the rotational anisotropy (dependence on θ and ϕ) of the PES influence its dynamics. On the corrugated surface, the surface-normal translational motion of the impinging H_2 couples with its surface-parallel translational motion, and the impinging H_2 exhibits off-specular scattering, while on the less corrugated surface (i.e., the nearly flat surface), the impinging H_2 exhibits specular scattering. However, these

corrugation effects in the scattering process also strongly depend on the rotational motion of the impinging H_2, i.e., whether the H_2 is exhibiting cartwheel-like rotation or helicopter-like rotation. Since the cartwheel-like rotating H_2 rotates on an axis parallel to the surface, it is mainly affected by the polar orientational (θ) dependence (anisotropy), which is included as '$\cos^2\theta$' terms in equation (2). According to the *ab initio* PES calculation results for H_2 on Cu(001) [39], as H_2 approaches the surfaces, the coefficient (of the '$\cos^2\theta$' terms) $V_{2000}(s)$ becomes large compared to $V_{2011}(s)$ and $V_{2010}(s)$ (see figure 1). This means that the cartwheel-like rotating H_2 is less susceptible to corrugation effects during the scattering process, because the $V_{2000}(s)$ term includes no corrugation term (i.e., no dependence on X and Y; see equation (2)). Therefore, the coupling between the surface-normal translational motion and the surface-parallel translational motion is very small, and the cartwheel-like rotating H_2 is mainly scattered in the specular direction. On the other hand, the helicopter-like rotating H_2 rotates on an axis perpendicular to the surface; thus it is strongly affected by the azimuthal orientational (ϕ) dependence (anisotropy), which is included as a '$\sin^2\theta\cos 2\phi$' term in equation (2). Since there is only one '$\sin^2\theta\cos 2\phi$' term in equation (2), and its coefficient $V_{2210}(s)$ (see figure 1) depends on the corrugation (i.e., dependence on X and Y), there is a strong coupling between the surface-normal translational motion and the surface-parallel translational motion of the helicopter-like rotating H_2 that occurs during the scattering process. Thus, helicopter-like rotating H_2 are mainly scattered in the off-specular direction.

To obtain the spatial distributions (orientational preference) of H_2 scattered from Cu(001), we calculate the quadrupole alignment factor $A_0^{(2)}(E_{tot})$, which is given by

$$A_0^{(2)}(E_{tot}) = \frac{\sum_{m_j}[3m_j^2 - j(j+1)]R^{m'n'}_{mnjm_j}(E_{tot})}{\sum_{m_j} j(j+1)R^{m'n'}_{mnjm_j}(E_{tot})}. \tag{4}$$

The quadrupole alignment factor $A_0^{(2)}(E_{tot})$ can be experimentally determined by using REMPI [10, 11] and LIF [13], and gives us information regarding the degree of alignment and orientational preference of H_2. It assumes values in the range $[-1, 3j/(j+1) - 1]$, i.e., cartwheel-like rotating H_2 ($m_j \approx 0$) has $A_0^{(2)}(E_{tot}) < 0$, while helicopter-like rotating H_2 ($|m_j| \approx j$) has $A_0^{(2)}(E_{tot}) > 0$. A spatially isotropic distribution of the angular momentum vector $\boldsymbol{j}$ is described by $A_0^{(2)}(E_{tot}) = 0$. In figure 3, we show the $A_0^{(2)}(E_{tot})$ as a function of the scattering angle Θ_f of H_2, which can be evaluated from the surface-normal translational energy and the surface-parallel translational energy of scattered H_2. In figures 3(a) and (b), the surface-parallel wavevector of the impinging H_2 is fixed at $\boldsymbol{K}_i = G(1, 0)$ along the [100] direction of Cu(001), which corresponds to the incident angle $\Theta_i \approx 10^\circ$ with respect to the surface normal. In figure 3(a), we can observe a strong rotational alignment of H_2 scattered from Cu(001), where the H_2 scattered from Cu(001) in the region of the scattering angle $\Theta_i - 20^\circ < \Theta_f < \Theta_i + 20^\circ$ exhibits $A_0^{(2)}(E_{tot}) < 0$, while the H_2 scattered from Cu(001) in the regions of the scattering angle $\Theta_f < \Theta_i - 20^\circ$ and $\Theta_f > \Theta_i + 20^\circ$ exhibits $A_0^{(2)}(E_{tot}) > 0$. A similar result can be seen for different E_{tot} (=0.4 [eV]) in figure 3(b).

These results indicate that the orientational preference varies with the scattering angle of H_2 from Cu(001), and we can obtain H_2 with aligned angular momentum vectors $\boldsymbol{j}$ through the scattering process. The microscopic mechanism of the rotational alignment of scattered H_2 can be attributed to the strong coupling between the surface-parallel translational motion and the rotational motion of H_2. A helicopter-like rotating H_2 is more susceptible to the surface corrugation than a cartwheel-like rotating H_2. Helicopter-like rotating H_2 are mainly affected by the azimuthal (ϕ) dependence of the PES, whereas cartwheel-like rotating H_2 are mainly affected by the polar (θ) dependence of the PES. Because of the generality of this behaviour,

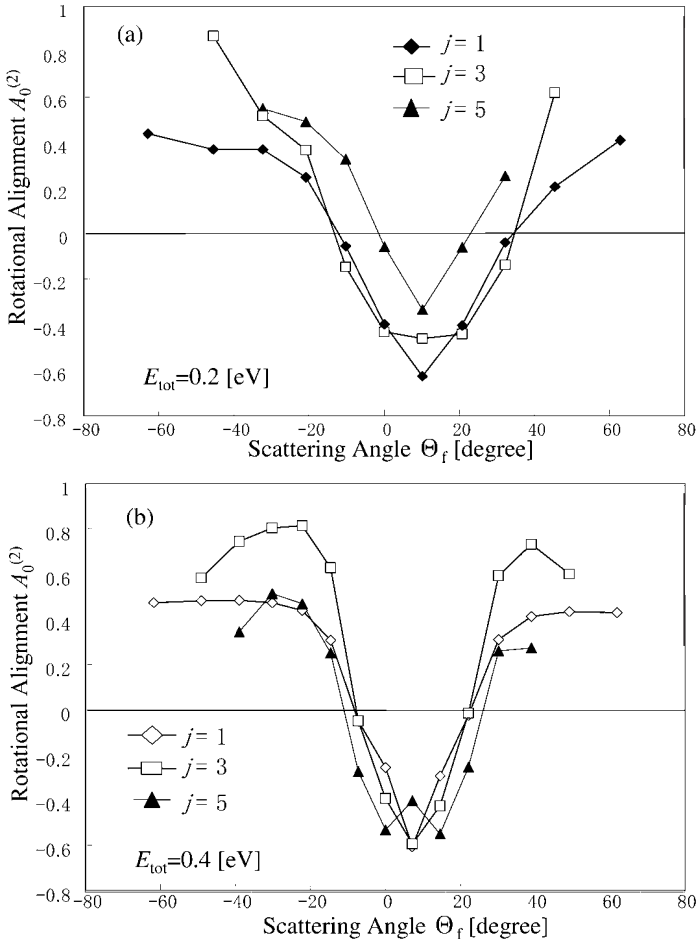

Figure 3. Rotational alignment $A_0^{(2)}(E_{tot})$ of H_2 scattered from Cu(001), in the vibrational ground state ($v = 0$), as a function of the final scattering angle along the [100] direction of Cu(001) for the cases when (a) $E_{tot} = 0.2$ [eV] and (b) $E_{tot} = 0.4$ [eV] for the rotational states $j = 1, 3, 5$.

we expect to observe a DQF effect on the scattering dynamics of other gas–surface systems. In general, a molecule which rotates on an axis parallel to the surface will exhibit specular scattering, while a molecule which rotates on an axis perpendicular to the surface will exhibit off-specular scattering.

In this letter, we investigated and discussed the effects of DQF on the scattering dynamics of H_2 on Cu(001). We have shown that due to the orientational dependence of hydrogen–surface interactions, surfaces may be utilized as filters to align the angular momentum vectors $\boldsymbol{j}$ of H_2. A cartwheel-like rotating H_2 will exhibit strong specular scattering, while a helicopter-like rotating H_2 will exhibit off-specular scattering. This can be attributed to the strong coupling between the surface-parallel translational motion and the rotational motion of H_2 during the scattering process. We thus conclude that the angular momentum vector $\boldsymbol{j}$ of freely rotating H_2 can be fixed/defined via the scattering angle of the H_2. Our calculation results can be verified by using available experimental techniques, such as the REMPI and LIF techniques, to observe the quadrupole alignment factor $A_0^{(2)}(E_{tot})$ for H_2

scattered from Cu(001) for different final scattering angles, such as $\Theta_i - 20^\circ < \Theta_f < \Theta_i + 20^\circ$ and $\Theta_f < \Theta_i - 20^\circ$ and $\Theta_f > \Theta_i + 20^\circ$.

We thank Dr Hiroshi Nakanishi for discussions and comments on this work. This work was partly supported by the Ministry of Education, Science, Sports and Culture of Japan through a Grant-in-Aid for COE Research (10CE2004), Scientific Research (C) (11640375, 13650026) programmes, the New Energy and Industrial Technology Development Organization (NEDO) through the Materials and Nanotechnology programme, the Japan Science and Technology Corporation (JST) through their Research and Development Applying Advanced Computational Science and Technology programme, and Toyota Motor Corporation through their Cooperative Research in Advanced Science and Technology. Some of the calculations presented here were done using the computer facilities of the JST, and the ISSP Supercomputer Centre (University of Tokyo). YM gratefully acknowledges a Fellowship grant from the JST through their Research and Development Applying Advanced Computational Science and Technology programme. WAD acknowledges support from the Marubun Research Promotion Foundation.

References

[1] Rettner C T, Auerbach D J and Michelsen H A 1992 *Phys. Rev. Lett.* **68** 2547
[2] Hodgson A, Moryl J, Traversaro P and Zhao H 1992 *Nature* **356** 501
[3] Rettner C T, Auerbach D J and Michelsen H A 1992 *Phys. Rev. Lett.* **68** 1164
[4] Michelsen H A, Rettner C T, Auerbach D J and Zare R N 1993 *J. Chem. Phys.* **98** 8294
[5] Rettner C T, Michelsen H A and Auerbach D J 1995 *J. Chem. Phys.* **102** 4625
[6] Gostein M and Sitz G O 1997 *J. Chem. Phys.* **106** 7378
[7] Murphy M J and Hodgson A 1997 *Surf. Sci.* **390** 29
[8] Murphy M J and Hodgson A 1998 *J. Chem. Phys.* **108** 4199
[9] Watts E and Sitz G O 1999 *J. Chem. Phys.* **111** 9791
[10] Gulding S J, Wodtke A M, Hou H, Rettner C T, Michelsen H A and Auerbach D J 1996 *J. Chem. Phys.* **105** 9702
[11] Hou H, Gulding S J, Rettner C T, Wodtke A M and Auerbach D J 1997 *Science* **277** 80
[12] Greene C H and Zare R N 1983 *J. Chem. Phys.* **78** 6741
[13] Wetzig D, Dopheide R, Rutkowski M, David R and Zacharias H 1996 *Phys. Rev. Lett.* **76** 463
[14] Diño W A, Kasai H and Okiji A 1995 *J. Phys. Soc. Japan* **64** 2478
[15] Gross A, Wilke S and Scheffler M 1995 *Phys. Rev. Lett.* **75** 2718
[16] Kroes G J, Baerends E J and Mowrey R C 1997 *J. Chem. Phys.* **107** 3309
[17] Diño W A, Kasai H and Okiji A 1997 *Phys. Rev. Lett.* **78** 286
[18] Dai J and Light J C 1998 *J. Chem. Phys.* **108** 7816
[19] Darling G R and Holloway S 1998 *Surf. Sci.* **400** 314
[20] McCormack D A, Kroes G J, Olsen R A, Baerends E J and Mowrey R C 1999 *J. Chem. Phys.* **110** 7008
[21] Miura Y, Kasai H, Diño W A and Okiji A 2000 *J. Phys. Soc. Japan* **69** 3878
[22] Diño W A, Fukutani K, Okano T, Kasai H, Okiji A, Farias D and Rieder K H 2001 *J. Phys. Soc. Japan* **70** 3491
[23] Miura Y, Kasai H, Diño W A and Okiji A 2002 *J. Phys. Soc. Japan* **71** 222
[24] Michelsen H A, Rettner C T and Auerbach D J 1994 *Springer Series in Surface Science* vol 1, ed R J Madix (Berlin: Springer) p 185
[25] Darling G R and Holloway S 1995 *Rep. Prog. Phys.* **58** 1595
[26] Gross A 1998 *Surf. Sci. Rep.* **32** 291
[27] Kroes G J 1999 *Prog. Surf. Sci.* **60** 1
[28] Hodgson A 2000 *Prog. Surf. Sci.* **63** 1
[29] Diño W A, Kasai H and Okiji A 2000 *Prog. Surf. Sci.* **63** 63
[30] Diño W A, Kasai H and Okiji A 1999 *Surf. Sci.* **427–8** 358
[31] Diño W A, Kasai H and Okiji A 1998 *J. Phys. Soc. Japan* **67** 1517
[32] Diño W A, Kasai H and Okiji A 1998 *Surf. Sci.* **418** L39
[33] Muhida R, Diño W A, Miura Y, Kasai H, Nakanishi H, Fukutani K, Okano T and Okiji A 2002 *J. Vac. Soc. Japan* at press

[34] Muhida R, Diño W A, Fukui A, Kasai H, Nakanishi H, Okiji A, Fukutani K and Okano T 2001 *Surf. Sci.* **285–91** 493
[35] Muhida R, Diño W A, Fukui A, Miura Y, Kasai H, Nakanishi H, Okiji A, Fukutani K and Okano T 2001 *J. Phys. Soc. Japan* **70** 3654
[36] Muhida R, Diño W A, Miura Y, Kasai H, Nakanishi H, Fukutani K, Okano T and Okiji A 2002 *Surf. Sci.* at press
[37] Rankin C C and Light J C 1969 *J. Chem. Phys.* **51** 1701
[38] Miura Y, Kasai H and Diño W A 1999 *J. Phys. Soc. Japan* **68** 887
[39] Wiesenekker G, Kroes G J and Baerends E J 1996 *J. Chem. Phys.* **104** 7344
[40] Hammer B, Scheffler M, Jacobsen K W and Nørskov J K 1994 *Phys. Rev. Lett.* **73** 1400
[41] White J A, Bird D M, Payne M C and Stich I 1996 *Phys. Rev. Lett.* **73** 1404
[42] Kratzer P, Hammer B and Nørskov J K 1996 *Surf. Sci.* **359** 45